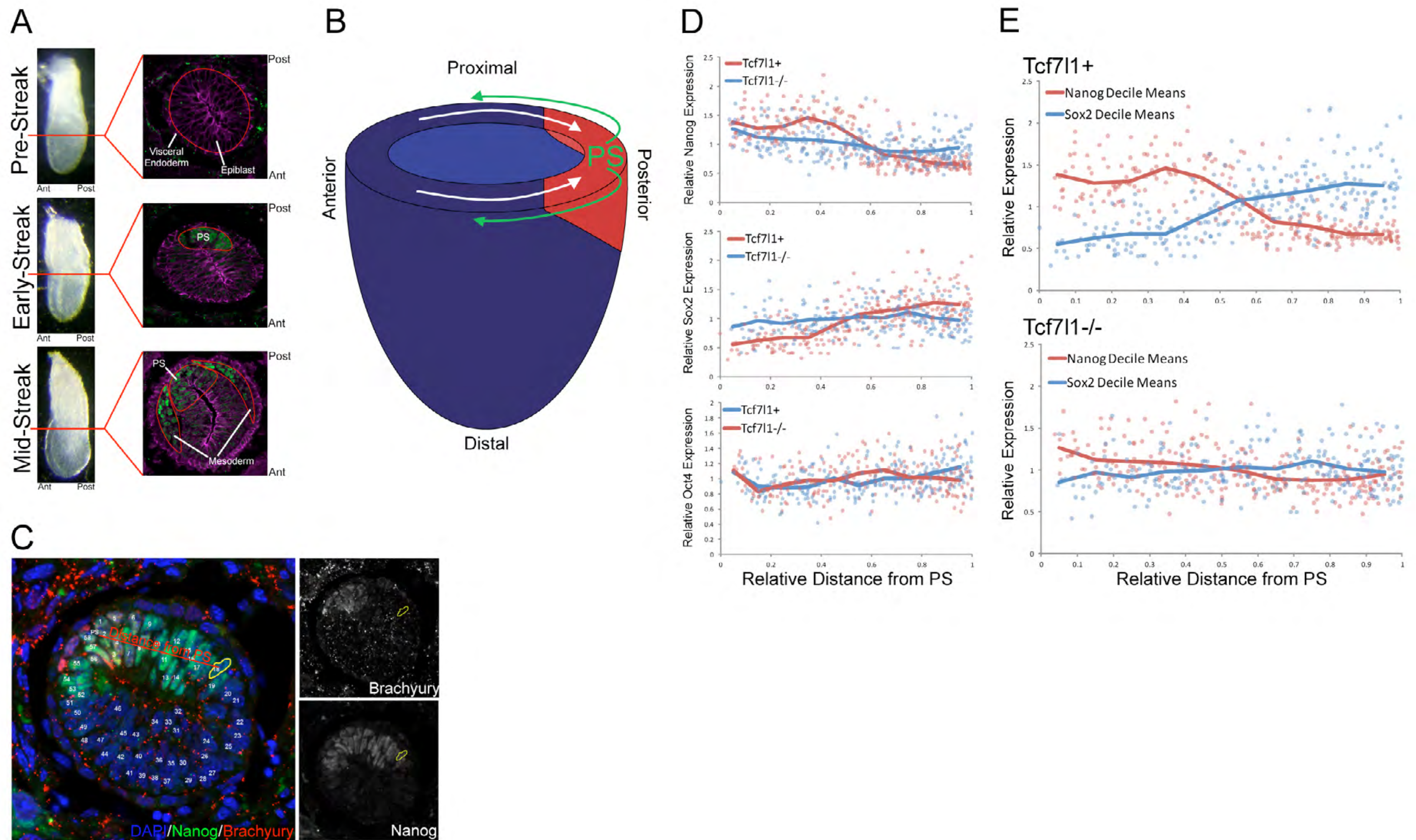

Fig. S1. Schematic of embryo staging, sectioning, cell movements and quantification of immunofluorescent staining. See also Figs 1 and 2. (**A**) Intact gastrulation stage embryos (left) were sectioned within their decidua along a transverse axis, illustrated with the red line, to generate an embryo section (right). Sections of embryos (right) are shown in the same orientation as in Fig. 1. These three images are identical to those in Fig. 1B-B″. Epiblast and visceral endoderm cells express membrane-associated E-cadherin (magenta) throughout gastrulation. Pre-streak embryos have an internal embryonic ectoderm layer (epiblast; enclosed by red oval) surrounded by the thin visceral endoderm, but do not have mesoderm forming at the PS. Early-streak embryos display a nascent PS structure (enclosed by red line) at the posterior, and activation of mesoderm gene expression (green). Mid-streak embryos have a PS structure, and mesoderm cells migrating laterally from the PS (red 'wings') lacking E-cadherin. Ant, anterior; post, posterior; PS, primitive streak. (**B**) Diagram of cell movements in the early streak epiblast summarized from several studies (Lawson et al., 1991; Tam et al., 1997). Movement of epiblast cells is depicted with white arrows, and movement of mesoderm cells is depicted with green arrows. During PS formation, cells in the proximal epiblast move from the anterior towards the posterior and enter into the PS where they specify mesoderm, exit the epiblast and form a new layer of mesoderm cells that migrate laterally towards the anterior. Cells in the distal anterior epiblast move proximally to replace the cells moving towards the posterior. (**C**) Example of an embryo used for quantification of immunofluorescent staining. Each nucleus in the epiblast was numbered and the middle of the PS was marked. The straight line distance from the PS to the center of each nucleus was measured. Each nucleus was then outlined and the mean intensity of signal in each RGB channel was determined. Nucleus 18 is outlined in yellow as an example measuring Nanog and brachyury nuclear intensities. (**D**) Overlay of immunofluorescent quantification from *Tcf7l1*$^{+}$ (red) and *Tcf7l1*$^{-/-}$ (blue) embryos depicted in Figs 1 and 2 for Nanog (top), Sox2 (middle) and Oct4 (bottom). Lines represent mean immunofluorescence intensities for nuclei grouped into ten deciles by distance from PS. (**E**) Overlay of immunofluorescence quantification of Nanog and Sox2 expression from *Tcf7l1*$^{+}$ (top) and *Tcf7l1*$^{-/-}$ (bottom) embryos from Figs 1 and 2. Lines represent mean immunofluorescence intensities for nuclei grouped into ten deciles by distance from PS. Note that the reciprocal patterns of Nanog and Sox2 immunofluorescence intensity are greatly reduced in *Tcf7l1*$^{-/-}$ embryos.

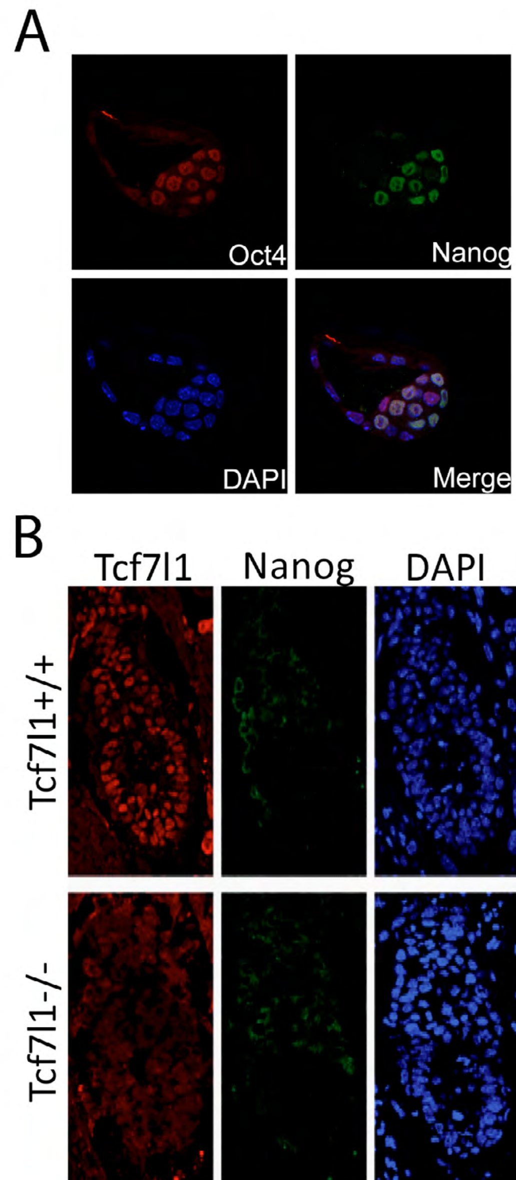

Fig. S2. Nanog and Oct4 expression in blastocysts and E5.5 embryos. (**A**) Confocal microscopy section through a representative of 40 blastocysts obtained from breeding *Tcf7l1*$^{+/-}$ mice. (**B**) Immunofluorescent staining for Tcf7l1 (red), Nanog (green) and nuclei (DAPI, blue) on sagittal sections of *Tcf7l1*$^{+}$ (top) and *Tcf7l1*$^{-/-}$ (bottom) embryos at E5.5.

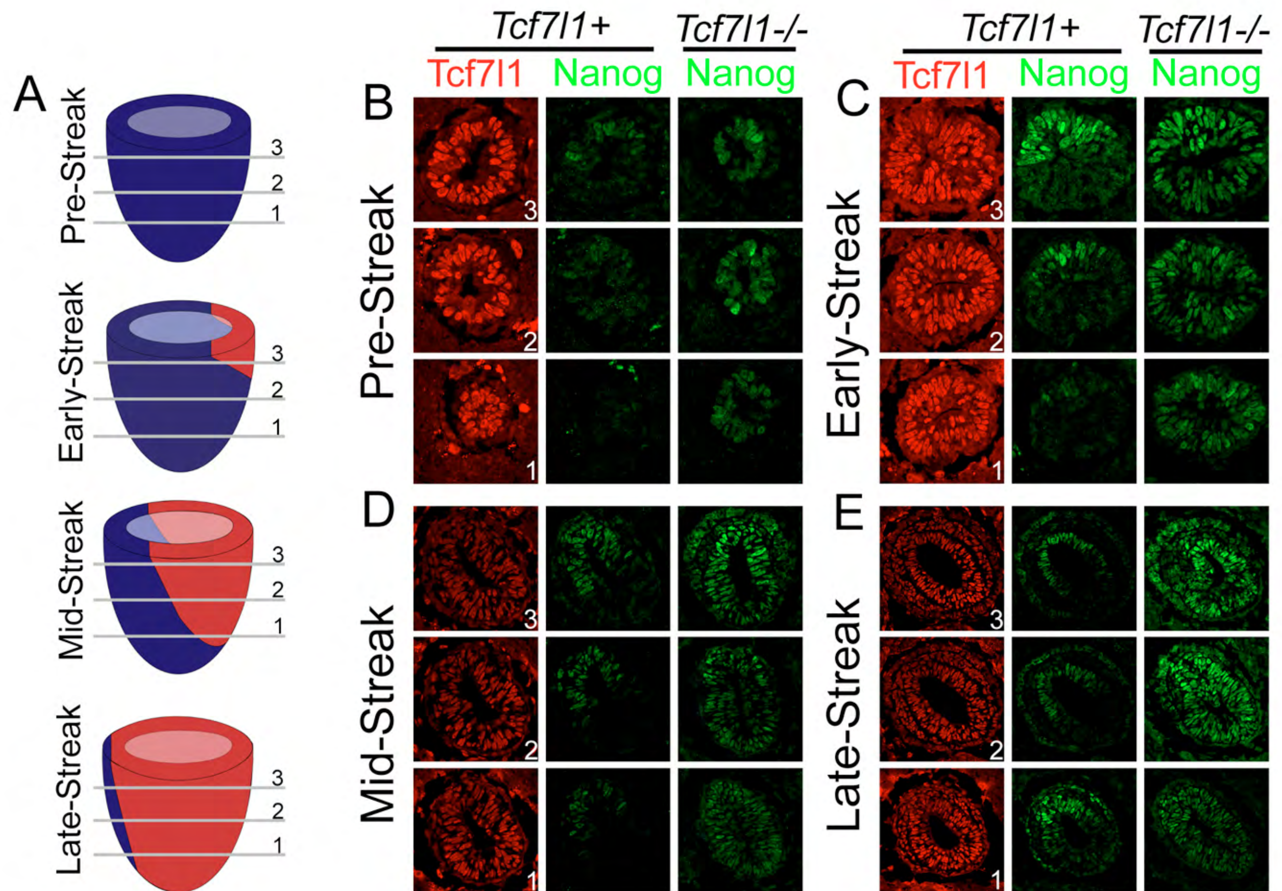

Fig. S3. Three-dimensional analysis of Nanog expression during PS formation. (**A**) In the schematic of experimental design (left), blue represents the epiblast and red represents the area covered by the PS and mesoderm. (**B-E**) Tcf7l1 (red) and Nanog (green) protein expression in *Tcf7l1*$^{+}$ and *Tcf7l1*$^{-/-}$ embryos at pre- (B), early- (C), mid- (D) and late- (E) streak stages. Numbers 1-3 correspond to the approximate position in the embryo shown in the schematic.

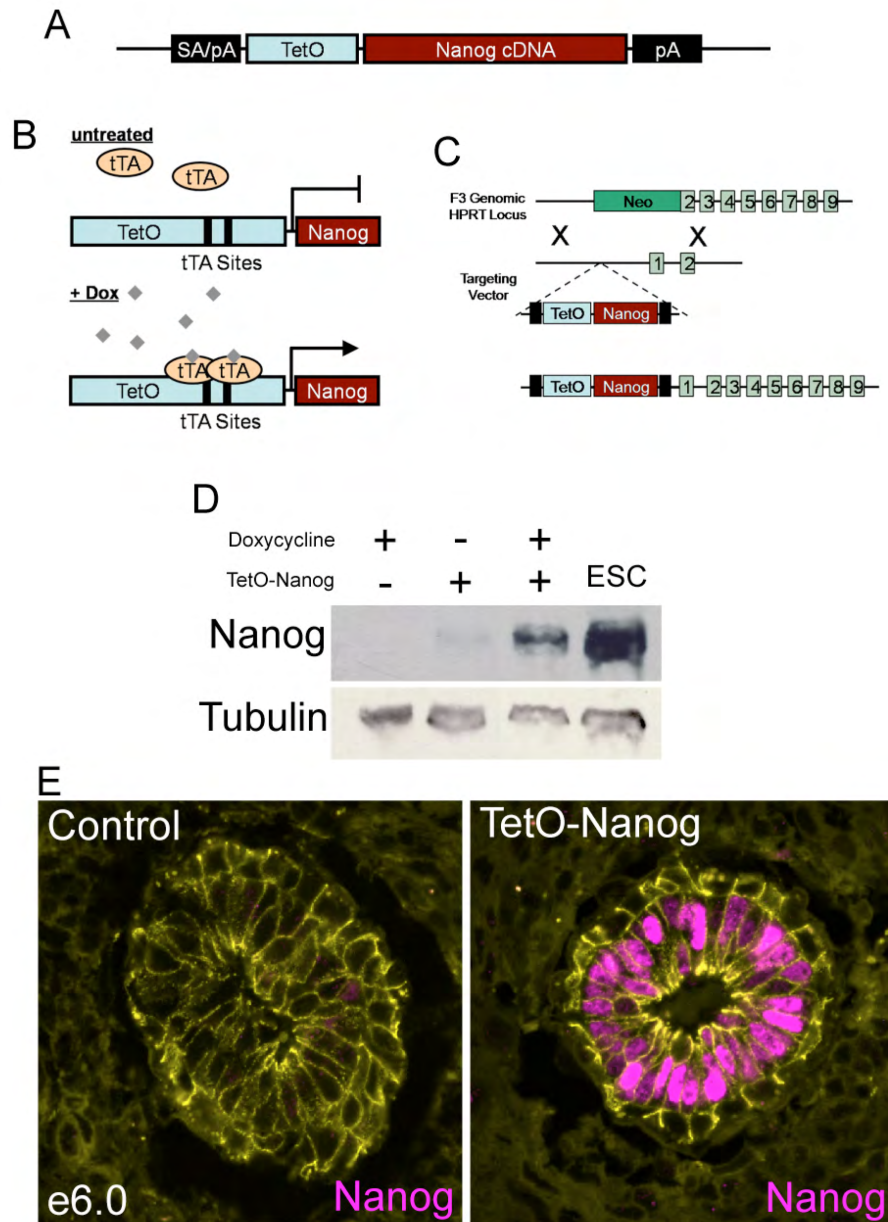

Fig. S4. Doxycycline-inducible *Nanog* transgenic mice. (**A**) Design of the TetO-Nanog gene cassette. Tet operator (TetO) and *Nanog* cDNA flanked by an upstream splice acceptor and polyadenylation signal sequence (SA/PA) and downstream polyadenylation signal sequence (PA). (**B**) Tet-On induction mechanism. In the absence of doxycycline, the Tet transactivator protein (tTA) is unable to bind to tTA target sequences in the TetO and Nanog expression is not induced. In the presence of doxycycline, the tTA protein binds to tTA target sequences in the TetO and promotes transcription of *Nanog* mRNA. (**C**) Genomic integration of the TetO-Nanog gene cassette by homologous recombination removes neomycin resistance and restores HPRT gene function in F3 cells. (**D**) Western blot for Nanog and tubulin in U2OS-tTA cells transfected with the TetO-Nanog targeting vector and treated with doxycycline. Note that Nanog expression was only induced in the presence of both doxycycline and the TetO-Nanog vector. ESC protein was included as a positive control for Nanog expression. (**E**) Immunofluorescent staining for Nanog (magenta) and E-cadherin (yellow) on transverse sections of doxycycline-induced control (left) and TetO-Nanog (right) embryos at E6.0. Note that Nanog is ectopically expressed throughout the epiblast of the TetO-Nanog embryo prior to induction of Nanog expression in the epiblast of the control embryo.

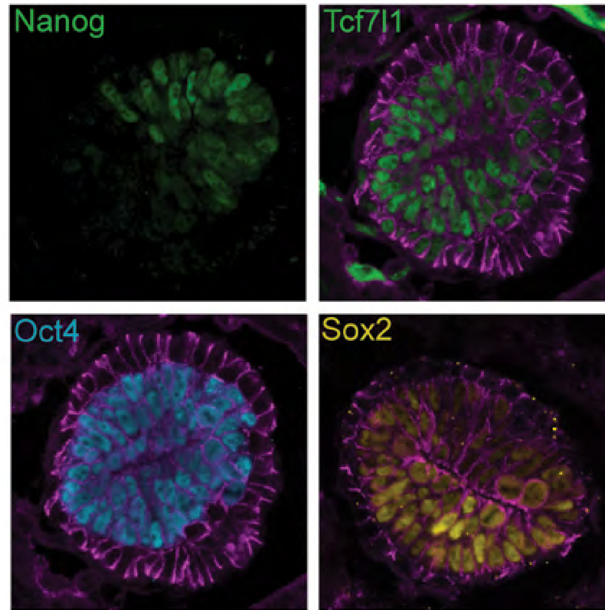

Fig. S5. Pluripotency factor expression in non-overexpressing *Nanog* transgenic controls. Immunofluorescent detection of Nanog, Tcf7l1, Oct4 and Sox2 protein in transverse sections of early-streak stage non-overexpressing *Nanog* transgenic controls. Note that the patterns of Nanog, Tcf7l1, Oct4 and Sox2 expression are indistinguishable from those in *Tcf7l1*$^{+/+}$ embryos (Fig. 1) and Nanog-overexpressing embryos (Fig. 2).

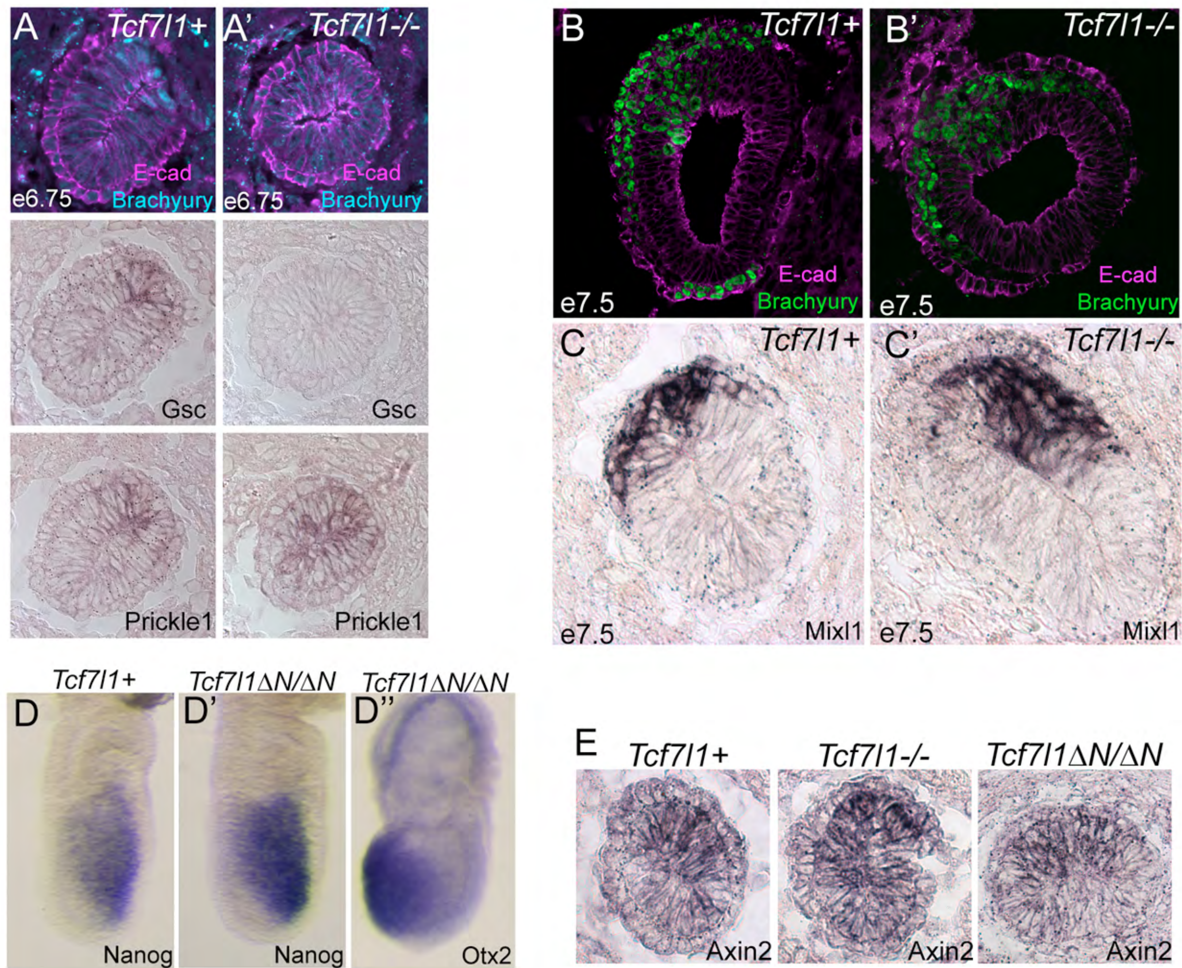

Fig. S6. Mesoderm genes are expressed in *Tcf7l1*$^{-/-}$ embryos after the delay and Tcf7l1/β-catenin interaction is not required for regulation of Nanog expression or Wnt/β-catenin mediated gene expression. (**A**,**A′**) Immunofluorescent detection of brachyury (cyan) and E-cadherin (magenta) and *in situ* hybridization of *Prickle1* and *Gsc* in early-streak *Tcf7l1*$^{+}$ (A) and *Tcf7l1*$^{-/-}$ (A′) embryos. (**B**,**B′**) Brachyury (green) and E-cadherin (magenta) immunofluorescent staining of a transverse section of an E7.5 *Tcf7l1*$^{+}$ (B) or *Tcf7l1*$^{-/-}$ (B′) embryo. Posterior is at the upper left of each image. Note that the anterior domain of brachyury expression detected in the prospective notochord of *Tcf7l1*$^{+}$ embryos is absent in *Tcf7l1*$^{-/-}$ embryos. (**C**,**C′**) *Mixl1* in situ hybridization on a transverse section of E7.5 *Tcf7l1*$^{+}$ (C) or *Tcf7l1*$^{-/-}$ (C′) embryo. Posterior is at the upper left of each image. (**D-D″**) Whole-mount *in situ* hybridization detection of *Nanog* (D,D′) and *Otx2* mRNA (D″) in *Tcf7l1*$^{+}$ and *Tcf7l1*$^{N/N}$ embryos. Each image is a lateral view of the embryo with posterior to the right. (**E**) *In situ* hybridization for *Axin2* on transverse sections of early-streak embryos. No reproducible difference was detected between *Tcf7l1*$^{+}$ (left), *Tcf7l1*$^{-/-}$ (middle) and *Tcf7l1*$^{N/N}$ (right) embryos. In each image, posterior is at the top.

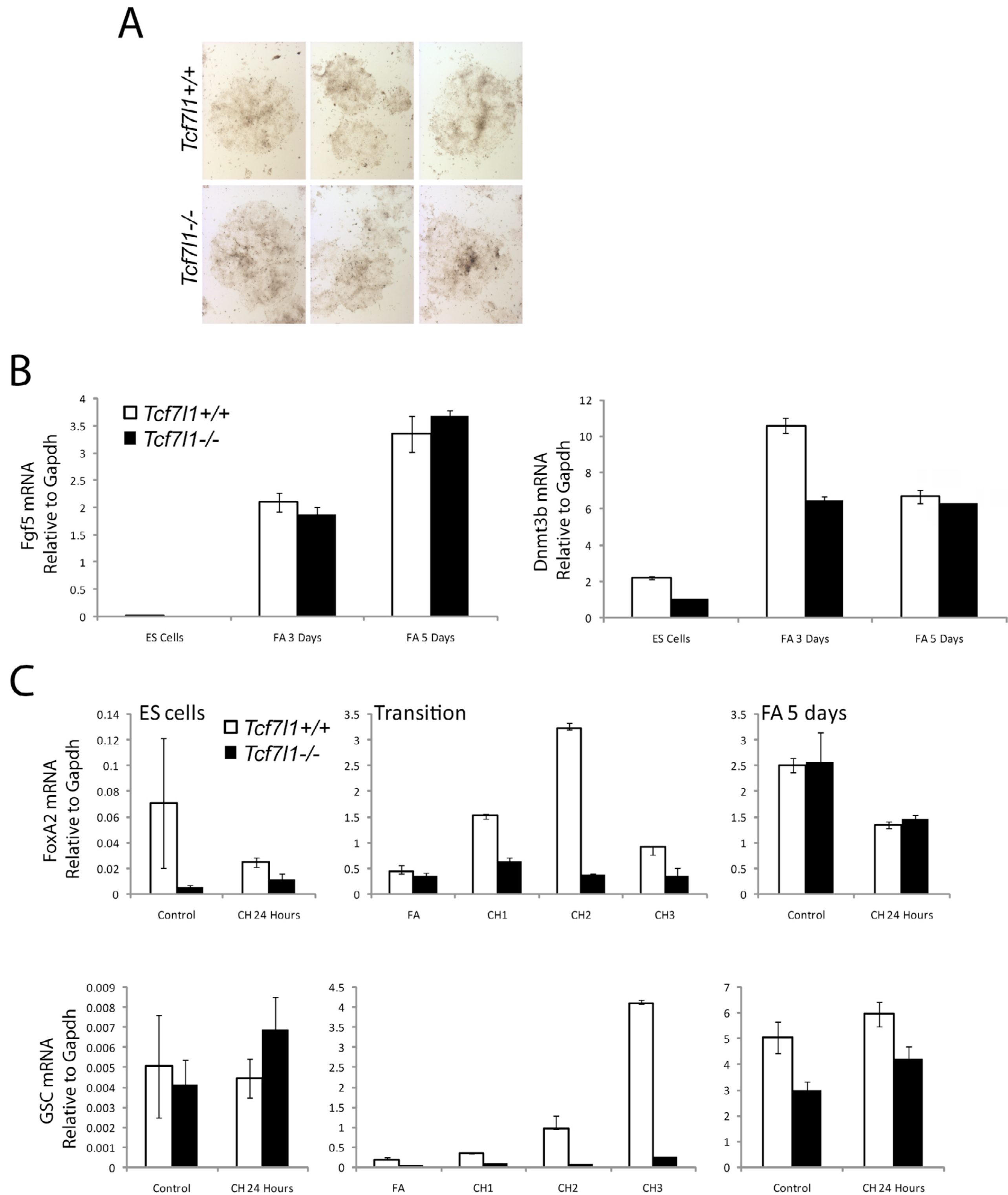

Fig. S7. Tcf7l1 is not required for induction of mesoderm gene expression. (**A**) Representative images of alkaline phosphatase-stained *Tcf7l1*$^{+/+}$ (top) and *Tcf7l1*$^{-/-}$ (bottom) colonies after 5 days in EpiSC culture conditions. Note that both *Tcf7l1*$^{+/+}$ and *Tcf7l1*$^{-/-}$ colonies are AP-negative and exhibit EpiSC-like colony morphology. (**B**) Quantitative RT-PCR assays measuring *Fgf5* and *Dnmt3b* mRNA expression relative to *Gapdh* in untreated ESCs and ESCs after 3 or 5 days in EpiSC conditions. (**C**) Quantitative RT-PCR assays measuring the levels of endoderm genes *Foxa2* (top) and *Gsc* (bottom) in response to CH in ESCs (left), in cells undergoing transition (middle), and in cells after 5 days of culture in EpiSC conditions (right) as in Fig. 6E. Values are normalized to the level of *Gapdh* expression in each sample. White bars represent *Tcf7l1*$^{+/+}$ cells and black bars represent *Tcf7l1*$^{-/-}$ cells.